Construction and Building Materials 25 (2011) 2122–2132

Contents lists available at ScienceDirect

Construction and Building Materials

journal homepage: www.elsevier.com/locate/conbuildmat

Comparison of accelerated climate ageing methods of polymer building materials by attenuated total reflectance Fourier transform infrared radiation spectroscopy

Bjørn Petter Jelle [a,b,*], Tom-Nils Nilsen [c]

[a] Department of Materials and Structures, SINTEF Building and Infrastructure, NO-7465 Trondheim, Norway
[b] Department of Civil and Transport Engineering, Norwegian University of Science and Technology (NTNU), NO-7491 Trondheim, Norway
[c] Department of Chemical Engineering, Norwegian University of Science and Technology (NTNU), NO-7491 Trondheim, Norway

ARTICLE INFO

Article history:
Received 27 August 2010
Received in revised form 4 November 2010
Accepted 13 November 2010
Available online 10 December 2010

Keywords:
Polypropylene, PP
High density polyethylene, HDPE
Accelerated climate ageing
Solar radiation
Ultraviolet radiation, UV
Attenuated total reflectance, ATR
Fourier transform infrared, FTIR

ABSTRACT

The degradation of the polymer building materials polypropylene (PP) and high density polyethylene (HDPE) intended for application as water barriers/repellants around building foundation walls have been studied. The PP and HDPE samples have been subjected to various accelerated climate ageing methods for comparison, including exposure to ultraviolet and infrared radiation, heated air, water spray and freezing. The climate ageing processes have been qualitatively and quantitatively investigated by attenuated total reflectance (ATR) Fourier transform infrared (FTIR) radiation spectroscopy.

1. Introduction

1.1. Climate exposure

The climate exposure represents a substantial strain on buildings and other structures subjected to outdoor conditions. This weathering strain consists of several individual climate exposure factors which may influence each other and the total outcome of the exposure, e.g. solar radiation, material expansions and contractions due to temperature fluctuations, freezing/thawing cycles, wind forces, water in the form of humidity in air and building materials, rain, driving rain and ground water pressure. The weathering may affect the buildings at both a material, component or structural level. Different materials will experience different exposure as they are used in different parts of a building, and they will have different resistance towards the various climate exposure factors.

1.2. Climate ageing and solar radiation

Climate ageing is a result from climate exposure, e.g. from solar radiation exposure. Solar radiation, in particular the high energy part of the solar spectrum, i.e. ultraviolet (UV) radiation, will damage organic materials depending on exposure level and time. Building materials like wood, plastic and paint might be vulnerable to various levels of solar radiation exposure. The photodamage in materials ranges from discolouration to loss of mechanical integrity. Several strategies are employed in order to protect against the solar deterioration. Organic building materials might be protected through the application of light stabilizers and/or surface treatment.

1.3. Accelerated artificial climate ageing

Various equipment are made in order to study the climate ageing processes in the laboratory within a reasonable timeframe. The ageing processes are therefore accelerated artificially, e.g. a process which takes 12 years during real life outdoor weather exposure may in laboratory take only 1 year. Ultraviolet and short-wave visible solar radiation initiate the degradation processes, while the actual chemical reaction rate increases exponentially with temperature. A combined acceleration factor may be calculated based upon the total ultraviolet exposure energy dosage (in J/m^2 or kWh/m^2) and accelerated ageing temperature. It is of uttermost importance not to subject the test samples to climate conditions which may initiate processes which will not occur during real climate exposure. For example, test samples are *not* to be irradiated with ultraviolet radiation with shorter wavelength (higher energy)

* Corresponding author at: Department of Materials and Structures, SINTEF Building and Infrastructure, NO-7465 Trondheim, Norway. Tel.: +47 73 593377; fax: +47 73 593380.
E-mail address: bjorn.petter.jelle@sintef.no (B.P. Jelle).

0950-0618/$ - see front matter © 2010 Elsevier Ltd. All rights reserved.
doi:10.1016/j.conbuildmat.2010.11.020

than occurs in nature, otherwise chemical bonds in the test samples may be broken which never will break during natural climate ageing. Likewise, one may want to apply as high temperature as possible in order to gain as high acceleration factor as possible, but the temperature must be kept below a certain critical temperature level where reactions that in nature will be negligible start to have significant influence. Generally, for accelerated climate ageing testing of most polymer materials, a temperature between 60 °C and 70 °C is often chosen. Furthermore, one should note that repeated freezing and thawing of building materials and components containing water may cause large degradations due to frost weathering and cracking during water to ice volume expansion, both at a macro and micro scale. In climates which experience many freezing point passes during freezing and thawing, it is very important to test the resistance and durability towards these freezing/thawing cycles. These aspects complicates furthermore any calculation of a total acceleration factor and the possibilities of lifetime predictions. Relative lifetime estimations and comparisons of samples are thus more feasible than absolute predictions of lifetimes.

1.4. FTIR analysis

A Fourier transform infrared (FTIR) radiation analysis yields a fingerprint of the material sample in question, and changes due to ageing processes, e.g. accelerated climate ageing, may be studied. That is, decomposition and formation of chemical bonds and products can be investigated in a FTIR analysis. Both qualitative and quantitative FTIR measurements may be performed and studies of chemical reactions and concentration changes are thus possible. Both solids, liquids and gases, including fast reactions, may be studied. In addition, biological growth, e.g. mould and fungus, may also be examined by FTIR analysis, as well as the impact on the attacked substrate material. Various aspects may complicate a FTIR analysis, e.g. the FTIR signals from the degradation products might be hidden behind the signals from the base (substrate) material, and several chemical reactions may be occurring at both the same time and at different times making it difficult to differentiate between them.

1.5. The ATR technique

The attenuated total reflectance (ATR) technique utilized in FTIR spectroscopical investigations makes it possible to measure chemical changes directly in the material surface and enables the study of materials in a pristine condition. The ATR technique requires none or only minor sample preparations, thus saving time and resources. In several cases, the ATR technique will be superior compared to more traditional FTIR techniques carried out by running transmission spectra through material samples dissolved in a suitable liquid or pressed into a thin KBr pellet.

1.6. Objective of this work

In this work we have studied how we can apply ATR–FTIR spectroscopical techniques in order to investigate the climate ageing processes of polymer building materials, with polypropylene (PP) and high density polyethylene (HDPE) as selected examples, comparing various accelerated climate ageing apparatuses. More specifically, the PP and HDPE materials employed in this investigation, are intended for application as water repellants (plate products) around building foundation walls. The reasons for including UV radiation in the accelerated ageing are that the products may be exposed to UV radiation during storage and prior to being covered, and that parts of the products may be exposed to UV radiation during the lifetime of the products. Possible long time benefits or outcome from such experiments could be early detection of started ageing processes, and, extrapolation of the ageing processes quantitatively and thereby estimation of the material product's effective lifetime, i.e. one may ultimately skip long time outdoor natural and accelerated artificial ageing exposure experiments, saving both time and costs. Furthermore, a correlation between various material properties, e.g. tensile strength, and FTIR spectra may be sought and found. That is, some material properties testing might be replaced with the less time-consuming and more cost-effective FTIR analysis. Successful accelerated artificial climate ageing and estimation of effective lifetime of materials, components and structures is of outmost importance in product development.

2. Polymer degradation by solar radiation in general

Solar degradation of organic materials may include chemical, physical or biological reactions resulting in bond scission of organic materials with subsequent chemical transformations. These processes may involve molecular branching and crosslinking, fragmentations of molecular main chain leading to changes in molecular weight, alterations due to splitting off low molecular weight species, unsaturated carbon double bonds (C=C) and oxygenated groups. The degradation mechanism is influenced by photodegradation, chemical degradation/oxidation processes, thermal degradation, mechanochemical degradation and physical ageing.

The actual photodegradation mechanisms for different materials may be very complicated and involving several reaction steps, where oxygen and other environmental influences may be crucial for the exact reaction course. As an example, a reaction set consisting of 91 elementary reactions and 58 different species was needed to reproduce the experimentally measured kinetics for the photodegradation of a model system simulating lignin yellowing, e.g. the observed light-induced discolouration of wood materials in buildings [1]. Quantitative spectroscopy, including both ultraviolet and infrared absorption measurements, in order to determine the effects of photodegradation of a polymer coating, is performed in a work by Croll and Skaja [2]. Furthermore, Gerlock and co-workers apply both ultraviolet and infrared spectroscopy to assess the weathering performance of different clearcoats [3].

Photodegradation, photooxidation and photostabilization of polymers have been summarized by Rånby and Rabek in an extensive work with plenty of examples, including detailed reaction equations [4]. Polymer photodegradation, collecting a vast number of detailed reaction mechanisms, is also treated in another comprehensive work by Rabek [5]. Detailed photodegradation mechanisms of several polymers and polymer groups, including a large number of general reaction equations in addition to the more specific reactions, have been collected by Rabek in yet another work [6]. Furthermore, a recent review by Kumar et al. [7] addresses nanoscale particles for polymer degradation and stabilization. Andrady et al. [8] have studied the effects of climate change and UVB on materials. Also note the solar material protection factor (SMPF) introduced and defined by Jelle et al. [9] in order to measure and calculate the capability of glass to protect indoor materials from degradation caused by solar radiation. For further details and information on miscellaneous degradation, weathering and accelerated ageing processes of polymers, e.g. polypropylene and polyethylene, some including FTIR and ATR–FTIR techniques, it is referred to the available literature, e.g. [10–29].

As a simplistic model for the photodegradation process, the solar radiation single photon energy need to be larger than the chemical bonding energy in the molecules or atomic lattices in order to break up the bonds. That is, a carbon–chloride (C—Cl) bond of 5.42×10^{-19} J (327 kJ/mol) may be broken by UV photons of wavelength 300 nm and energy 6.63×10^{-19} J (4.14 eV), but not by light of wavelength 400 nm (border UV/VIS) and energy

4.97×10^{-19} J (3.11 eV). For calculations of photon energy, recall the relationship:

$$E = h\nu = hc/\lambda \quad (1)$$

where E denotes the photon energy, h the Planck constant (6.63×10^{-34} Js), ν the photon frequency, λ the photon wavelength and c the light velocity (3.00×10^{8} m/s). The Avogadro number N_A (6.02×10^{23} mol^{-1}) and the elementary (electron) charge e (1.60×10^{-19} C) may be applied in various of these calculations. Reorganization of Eq. (1) yields:

$$\lambda_{threshold} = hc/E_{threshold} \quad (2)$$

where $\lambda_{threshold}$ and $E_{threshold}$ denote the threshold photon wavelength and energy, where wavelengths below and energies above, will break the actual chemical bond, respectively, e.g. 367 nm and 327 kJ/mol for C—Cl.

The exact composition and structure of the various materials on an atomic level will determine the exact photon energy required to break up the bonds, e.g. one or more hydrogen atoms bonded to the same carbon atom as the chloride atom in the example above, may increase the bonding energy, i.e. CH_3—Cl (343 kJ/mol) has a larger bonding energy than C—Cl (327 kJ/mol). Impurities in the materials may also be responsible for absorption of light at higher wavelengths.

3. Experimental

3.1. Test material samples

Test samples of polypropylene (PP) and high density polyethylene (HDPE) intended for use as building foundation wall water barrier/repellant were cut in suitable sample sizes of approximately 2.5 cm × 2.5 cm.

3.2. QUV – QUV apparatus

A QUV apparatus, Weathering Tester Horizontal Option with Ponding and Water Spray (The Q-Panel Company, Cleveland, Ohio, USA), has been employed in order to subject the samples to UV radiation at a constant air temperature of 50 °C. The UVA and UVB intensities are averaged to 28 W/m^2 and 2.8 W/m^2 for the investigations reported within this work, respectively. No water spray was applied. The shortened form QUV is applied throughout the text as an abbreviation for this specific exposure.

3.3. Heat – heat incubator

A heat incubator (Termaks) has been employed in order to subject the samples to a constant air temperature of 90 °C. Note that this temperature of 90 °C is considerably higher than the normally accepted high-end safe temperature range between 60 °C and 70 °C. The higher temperature of 90 °C is chosen in order to test the actual materials for as high temperature as 90 °C and to accelerate the temperature degradation as much as possible (Arrhenius equation). The shortened form Heat is applied throughout the text as an abbreviation for this specific exposure.

3.4. Simul – vertical accelerated climate simulator

Accelerated weather ageing has been carried out in a vertical climate simulator according to Nordtest Method NT Build 495 (“Building materials and components in the vertical position: Exposure to accelerated climatic strains”) [30]. In this test equipment the samples are subjected in turns to four different climate zones, that is, one UV and IR irradiation zone (black panel temperature of 63 °C), one water spray zone (15 dm^3/(m^2 h)), one freezing zone (−20 °C) and one ambient laboratory climate zone. The UVA and UVB intensities are averaged to respectively 15 W/m^2 and 1.5 W/m^2 for the investigations reported within this work. The exposure time is 1 h in each climate zone in the above given sequence. For further details it is referred to the test method (NT Build 495). The shortened form Simul is applied throughout the text as an abbreviation for this specific exposure.

3.5. UV measurements

The UV measurements were carried out using a radiometer/photometer Model IL 1400A (International Light) with an UVA sensor and an UVB sensor.

3.6. FTIR material characterization

The FTIR material characterization was carried out with a Thermo Nicolet 8700 FTIR spectrometer with a Smart Orbit accessory, i.e. a horizontal attenuated total reflectance (ATR) accessory (single reflection) with a diamond crystal, in the wavelength range 4000 cm^{-1} (2.5 μm) to 400 cm^{-1} (25 μm) in an atmosphere with minimalized CO_2 and H_2O content through purging by a Parker Balston 74-5041 FTIR Purge Gas Generator. Each FTIR spectrum presented is based on a recording of 32 scans at a resolution of 4 cm^{-1}. In order to ensure satisfactory contact between the ATR diamond crystal and the sample, three or more FTIR spectra were recorded at various locations on the sample. The polymer surfaces are relatively hard, which complicates accurate quantitative measurements (height of absorbance peaks) due to varying contact with the ATR crystal for the different samples. Air between sample and ATR crystal results in a weaker absorbance signal. Unless other conditions indicate otherwise (e.g. inhomogenities, impurities, etc.), the FTIR curves with the largest absorbance peaks represent the most correct measurements on one and the same sample with equal ageing time, and hence these curves are chosen as they are assumed to be the most correct ones. Qualitative measurements (location of absorbance peaks at wave numbers) do not represent a problem as long as the contact area is large enough to ensure a sufficient strong measurement signal. The FTIR spectra given in this work have not been ATR corrected, neither with respect to penetration depths nor absorbance band shifts, which both are dependent on the refractive indices of the sample and the ATR crystal (diamond in this case) and the angle of incident radiation. The penetration depth is in addition also dependent on the radiation wavelength, and increases with increasing wavelength (decreasing wave number). That is, non-corrected ATR spectra have much stronger absorbance bands at longer wavelengths (smaller wave numbers) than at shorter wavelengths (larger wave numbers). Note that it should always be stated if an ATR–FTIR spectrum has been ATR corrected or not, e.g. important during computerized database spectra comparison searches. As we in this work is solely comparing the ATR–FTIR spectra measured within this work, there is no need for performing any ATR corrections. Besides, the raw ATR–FTIR data in either transmittance or logarithmic absorbance mode is usually preferred. It should also be noted that one often do not know the refractive indices of the samples which are measured, thus errors might be introduced in the ATR corrected spectra as the refractive index of the sample is an input parameter in the ATR correction.

4. Results and discussion

4.1. FTIR spectra

Various measured FTIR spectra with either transmittance or absorbance versus wave number are presented in Figs. 1–12. From

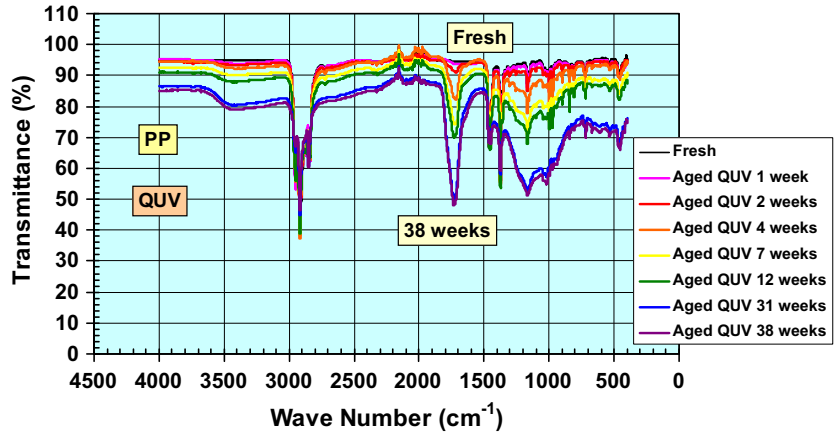

Fig. 1. Transmittance versus wave number between 4000 and 400 cm^{-1} for PP during QUV exposure.

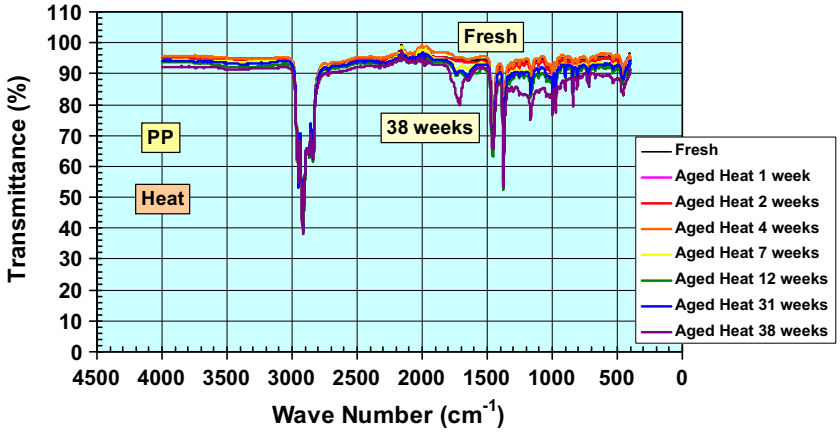

Fig. 2. Transmittance versus wave number between 4000 and 400 cm^{-1} for PP during Heat exposure.

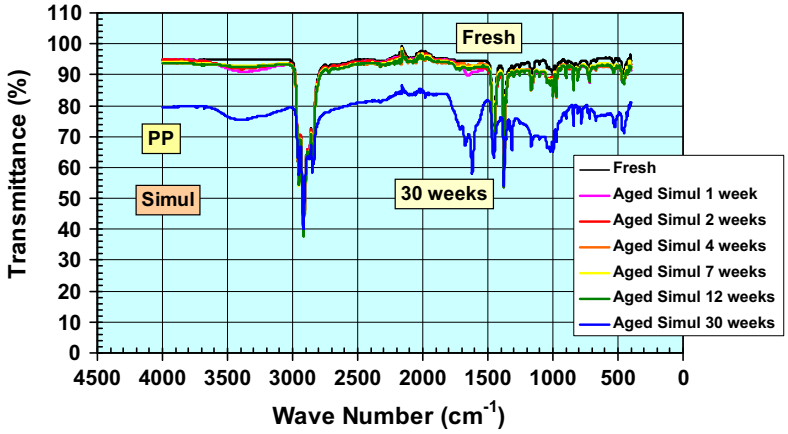

Fig. 3. Transmittance versus wave number between 4000 and 400 cm^{-1} for PP during Simul exposure.

these spectra an absorbance difference is calculated at specific wave numbers and plotted versus accelerated ageing time in Figs. 13–17. For easy comparison between the various transmittance spectra and between the various absorbance spectra, all the spectra are plotted with the same transmittance axis and the same absorbance axis, although this implies less spectra distinction from the paper plots for the cases with less accelerated ageing changes.

4.2. Logarithmic absorbance scale

As the absorption of electromagnetic radiation, e.g. IR radiation, follows the Beer–Lambert law, i.e. the radiation is decreasing exponentially with the penetration depth in the actual material, it is often helpful to plot the spectra on a logarithmic absorbance scale versus wavelength or wave number. Hence, a representative

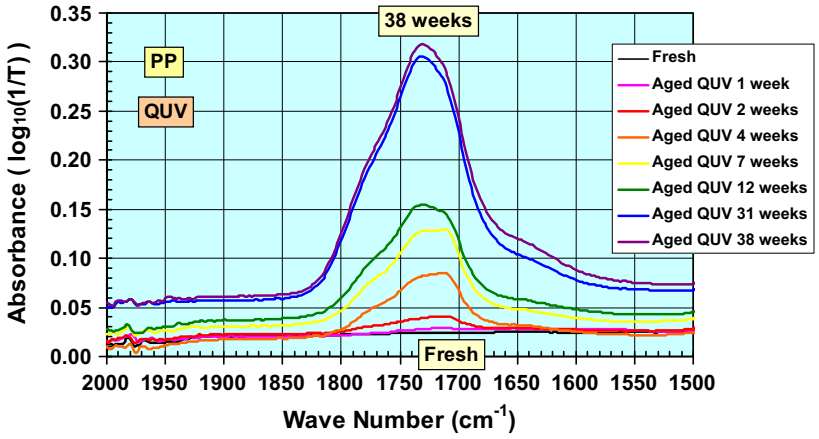

Fig. 4. Absorbance (logarithmic) versus wave number between 2000 and 1500 cm^{-1} for PP during QUV exposure.

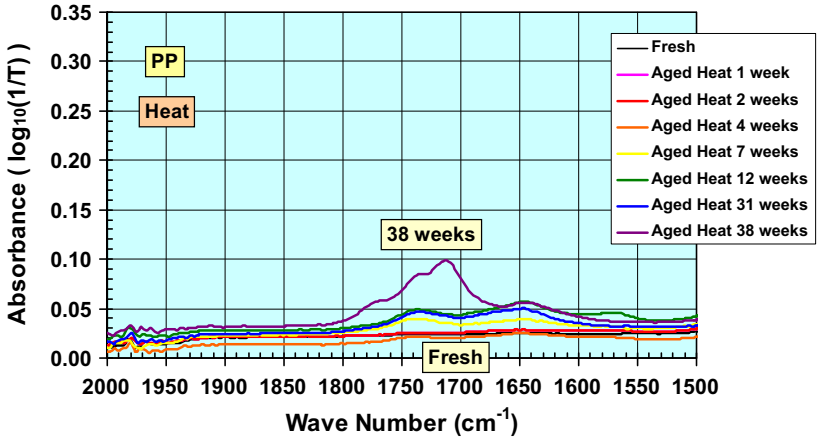

Fig. 5. Absorbance (logarithmic) versus wave number between 2000 and 1500 cm^{-1} for PP during Heat exposure.

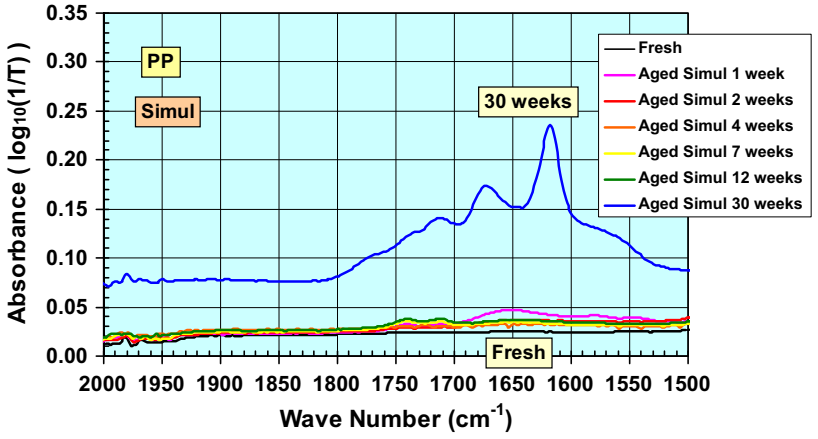

Fig. 6. Absorbance (logarithmic) versus wave number between 2000 and 1500 cm^{-1} for PP during Simul exposure.

spectrum is chosen from each of the samples and plotted on a logarithmic absorbance scale for quantitative studies. Mathematically and physically it follows that a doubling of the logarithmic absorbance, also called optical density, is interpreted as a doubling of material thickness or a doubling of concentration of absorption active agents.

4.3. Chemical reactions and absorption active species

The accelerated ageing exposure which makes the sample material undergo chemical changes (e.g. due to UV degradation) may then as a result of the chemical reactions change the actual thickness of the sample. In this work the experiments are per-

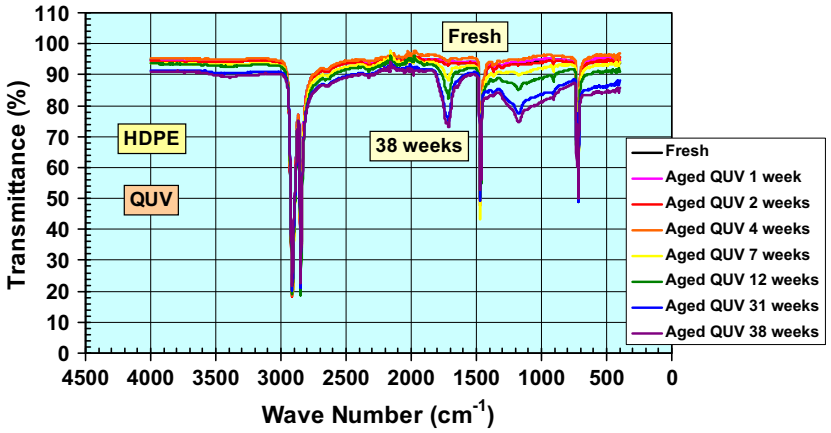

Fig. 7. Transmittance versus wave number between 4000 and 400 cm^{-1} for HDPE during QUV exposure.

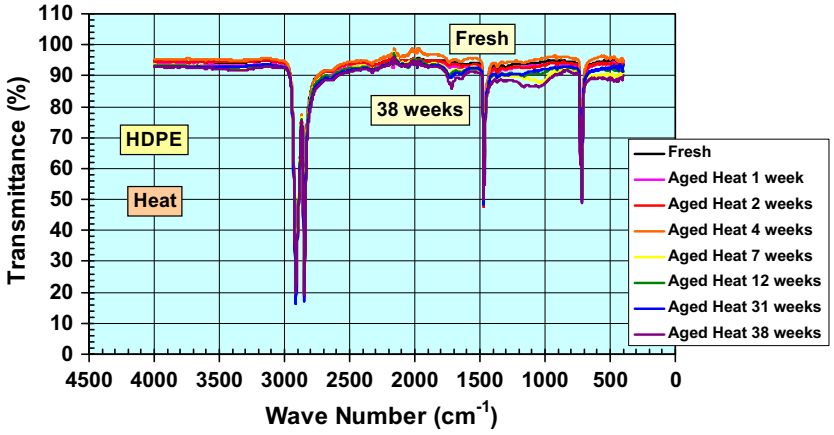

Fig. 8. Transmittance versus wave number between 4000 and 400 cm^{-1} for HDPE during Heat exposure.

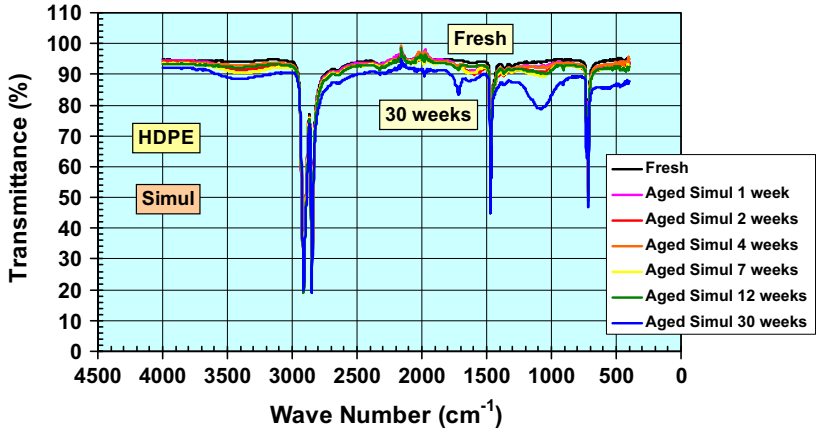

Fig. 9. Transmittance versus wave number between 4000 and 400 cm^{-1} for HDPE during Simul exposure.

formed applying the ATR equipment with the FTIR spectrometer. Hence, the IR radiation is only penetrating into a thin surface layer of the actual sample. With respect to the experiments carried out in this work, the material thickness will then be regarded as approximately constant, i.e. the change in the IR absorbance is explained by an increase or decrease of absorption active species within the sample material undergoing the chemical transformation.

4.4. Subdivisions of graphical FTIR spectra plots

FTIR transmittance spectra (measured with ATR equipment) in the wavelength range 4000 cm^{-1} (2.5 μm) to 400 cm^{-1} (25 μm) for PP at various accelerated ageing times in the QUV apparatus are shown in Fig. 1. More detailed views of these spectra plotted on a logarithmic absorbance scale in the wavelength range 2000 cm^{-1} (5 μm) to 1500 cm^{-1} (6.7 μm) are de-

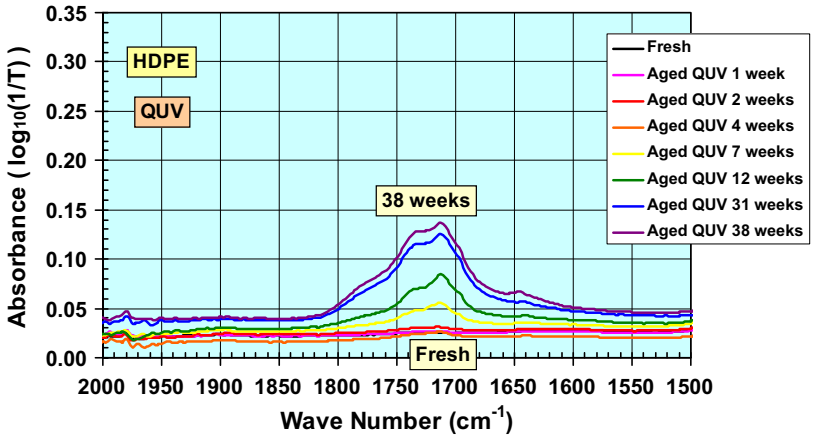

Fig. 10. Absorbance (logarithmic) versus wave number between 2000 and 1500 cm^{-1} for HDPE during QUV exposure.

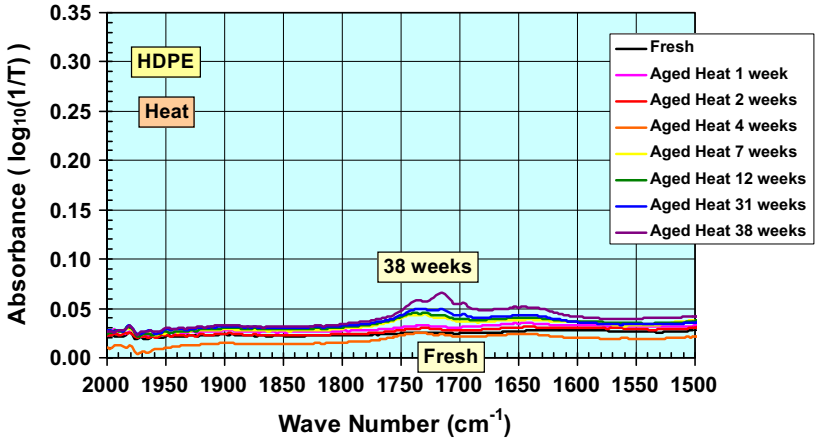

Fig. 11. Absorbance (logarithmic) versus wave number between 2000 and 1500 cm^{-1} for HDPE during Heat exposure.

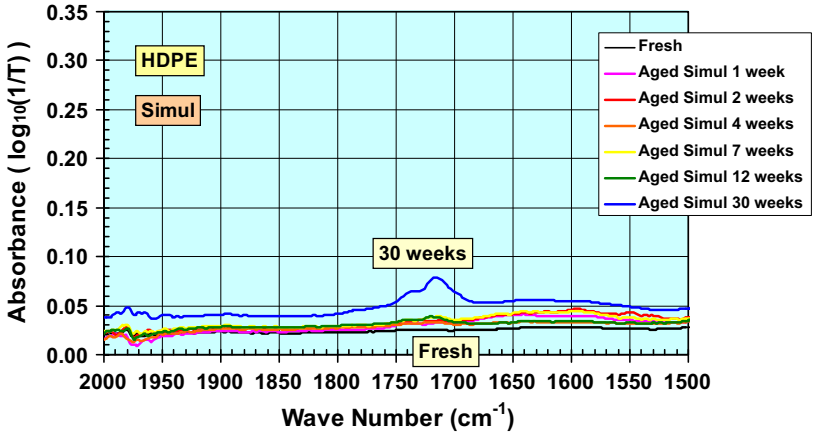

Fig. 12. Absorbance (logarithmic) versus wave number between 2000 and 1500 cm^{-1} for HDPE during Simul exposure.

picted in Fig. 4. Likewise, for PP in the Heat and Simul apparatuses, FTIR spectra are shown in Figs. 2 and 3 (transmittance) and Figs. 5 and 6 (detailed absorbance). Furthermore, likewise, for HDPE in the QUV, Heat and Simul apparatuses, FTIR spectra are shown in Figs. 7–12.

4.5. Graphical plots at specific wave numbers

In order to visualize the material changes in PP and HDPE with the accelerated ageing in the QUV, Heat and Simul apparatuses, the FTIR absorbance difference at specific wave numbers

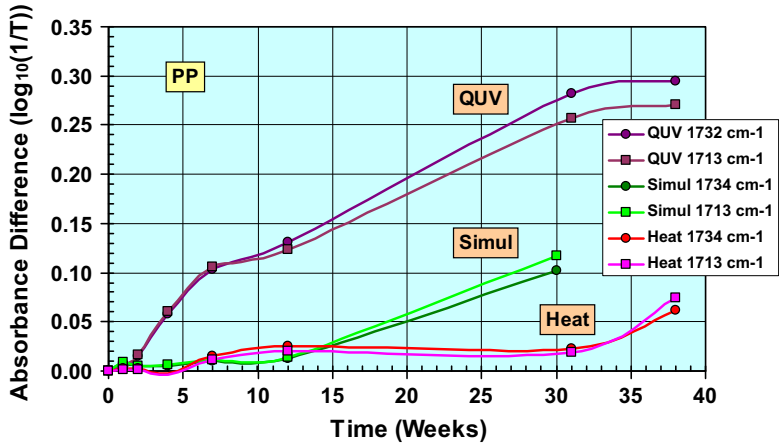

Fig. 13. Absorbance difference (logarithmic) versus exposure time for PP at wave numbers around 1732 cm^{-1} and 1713 cm^{-1} for the various accelerated ageing apparatuses.

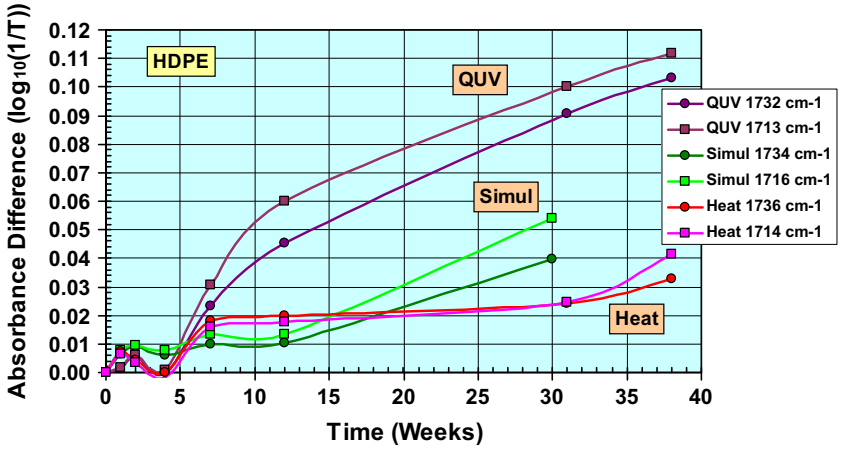

Fig. 14. Absorbance difference (logarithmic) versus exposure time for HDPE at wave numbers around 1732 cm^{-1} and 1713 cm^{-1} for the various accelerated ageing apparatuses.

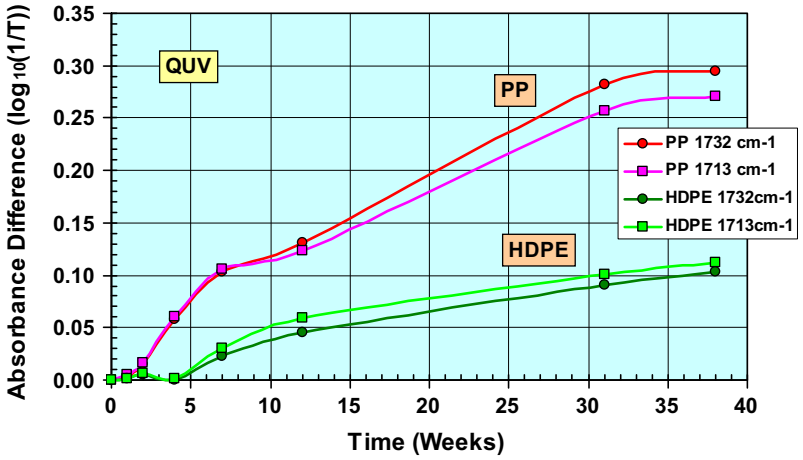

Fig. 15. Absorbance difference (logarithmic) versus exposure time for PP and HDPE at wave numbers around 1732 cm^{-1} and 1713 cm^{-1} for the QUV accelerated ageing apparatus.

is plotted versus the accelerated ageing time in Figs. 13–17. In this case the large absorbance change (for most cases) at wave numbers around 1732 cm^{-1} and 1713 cm^{-1} (with some variations) is chosen.

4.6. Comparing QUV, Heat and Simul exposure for PP and HDPE

Fig. 13 shows the absorbance difference versus accelerated ageing time for PP for QUV, Heat and Simul exposure, i.e. a direct com-

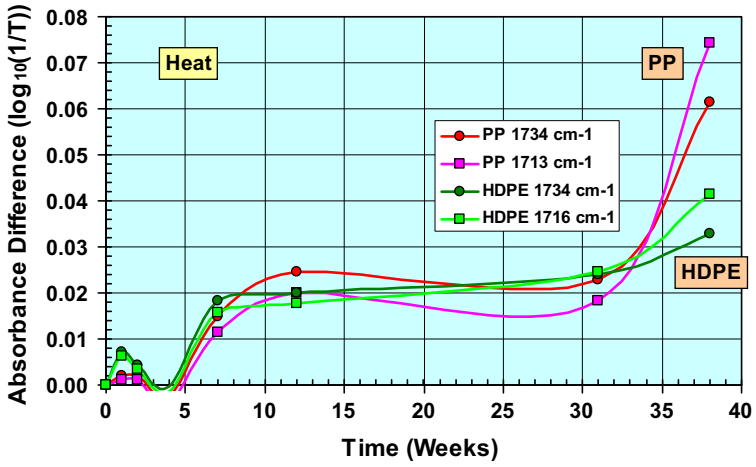

Fig. 16. Absorbance difference (logarithmic) versus exposure time for PP and HDPE at wave numbers around 1732 cm^{-1} and 1713 cm^{-1} for the Heat accelerated ageing apparatus.

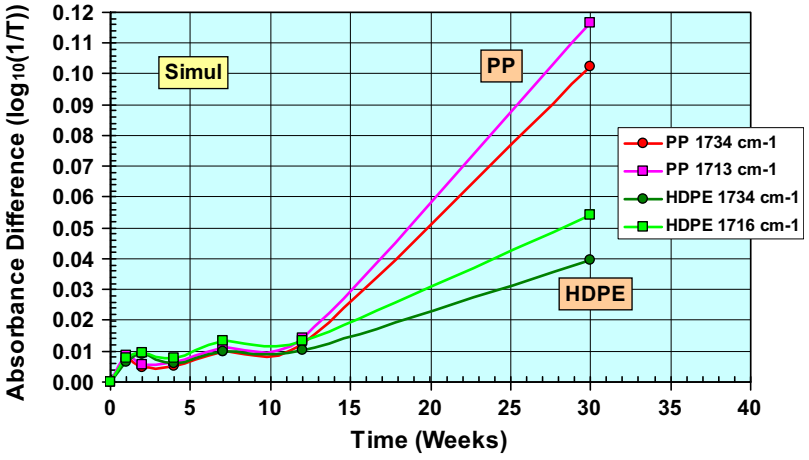

Fig. 17. Absorbance difference (logarithmic) versus exposure time for PP and HDPE at wave numbers around 1732 cm^{-1} and 1713 cm^{-1} for the Simul accelerated ageing apparatus.

parison of the three ageing apparatuses for the ageing in PP. Likewise, Fig. 14 shows the absorbance difference versus accelerated ageing time for HDPE for QUV, Heat and Simul exposure.

4.7. Comparing PP and HDPE for QUV, Heat and Simul exposure

Fig. 15 depicts the absorbance difference versus accelerated ageing time for PP and HDPE for QUV exposure, i.e. a comparison of PP and HDPE ageing for QUV exposure. Likewise, Fig. 16 depicts the absorbance difference versus accelerated ageing time for PP and HDPE for Heat exposure. Furthermore, likewise, Fig. 17 depicts the absorbance difference versus accelerated ageing time for PP and HDPE for Simul exposure.

4.8. ATR diamond large absorption

Note that the irregularities in the FTIR spectra between 2200 and 1900 cm^{-1} are due to the very large absorption in the ATR diamond crystal between these wave numbers, which represents the weak point in an otherwise excellent material crystal choice for ATR applications. Fortunately, only a limited number of chemical bonds have spectral absorption bands in this region.

4.9. Microscope photos

Microscope photos of non-aged PP and QUV aged for 38 weeks PP are shown in Fig. 18, clearly depicting the formation of cracks or crevices in the QUV aged PP. These cracks were not observed in PP aged by the other methods (Heat and Simul), neither in HDPE aged by all three methods (QUV, Heat and Simul), at a magnification of 90 x.

4.10. FTIR absorbance peaks

By inspecting Figs. 1–3 (PP) and Figs. 7–9 (HDPE) it is seen that due to the ageing processes large absorbance peaks are growing up at wave numbers around 1732 cm^{-1} and 1713 cm^{-1} ("the narrow 1700 cm^{-1} peak") and around 1200 cm^{-1} and 1000 cm^{-1} ("the broad 1100 cm^{-1} peak"). For HDPE two differences are noted: For the QUV exposure of HDPE, the peak is mainly located around 1200 cm^{-1} with no clear distinctive peak around 1000 cm^{-1}, while for the Simul exposure of HDPE the peak is mainly located around 1100 cm^{-1} with no clear distinctive peaks around 1200 cm^{-1} and 1000 cm^{-1}. In order to limit the number of figures in this article, only "the narrow 1700 cm^{-1} peak" is replotted in close-up graphs, Figs. 4–6 (PP) and Figs. 10–12 (HDPE).

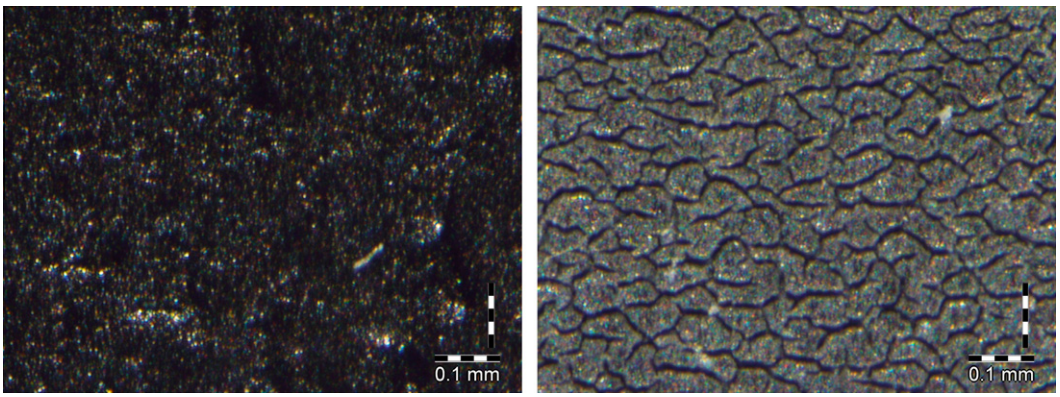

Fig. 18. Microscope photos of non-aged PP (left) and QUV aged for 38 weeks PP (right), clearly depicting the crevice formation in the QUV aged PP.

4.11. C=O and C—O oxidation

The peaks around 1732 cm^{-1} and 1713 cm^{-1} are attributed to carbonyl (C=O) stretching, i.e. an oxidation of the polymer occurs during UV and/or heat exposure in the QUV apparatus (QUV), heat incubator (Heat) and vertical accelerated climate simulator (Simul). The peaks around 1200 cm^{-1} and 1000 cm^{-1} are probably also due to oxidation processes, e.g. formation of C-O bonds.

4.12. Peak inspections and comparisons

It is observed that the carbonyl absorbance peaks for PP are substantially larger than the carbonyl absorbance peaks for HDPE for both QUV, Heat and Simul exposure. Furthermore, it is also observed that the carbonyl absorbance peaks for the QUV exposure are substantially larger than the carbonyl absorbance peaks for the Heat and Simul exposure for both PP and HDPE. In addition, for the Simul exposure, a large increase in the carbonyl absorbance peaks occurs between accelerated ageing times of 12 weeks and 30 weeks for both PP and HDPE. This may be due to increased surface area caused by freeze/thaw cycles. Finally, for the Simul exposure of PP two large absorbance peaks are observed at 1672 cm^{-1} and 1618 cm^{-1} for the ageing time of 30 weeks, which also are larger than the corresponding carbonyl absorbance peaks located above wave numbers of 1700 cm^{-1}. These absorbance peaks at 1672 cm^{-1} and 1618 cm^{-1} are not observed for the Simul exposure of HDPE. The origin of these peaks is at this stage not identified. All these miscellaneous comparisons are readily performed by inspecting the FTIR transmittance and absorbance spectra versus wave number in Figs. 1–12 and the absorbance difference calculated at specific wave numbers versus accelerated ageing time in Figs. 13–17.

4.13. Further details and comparisons

That is, the specific PP sample applied in these experiments is substantially more degraded by formation of carbonyl groups than the specific HDPE sample for all the accelerated climate exposures, i.e. QUV, Heat and Simul. This is probably explained by the fact that PP is more prone to be susceptible for UV photon attacks due to the alternating —CH_3 groups in the PP chain. Furthermore, the QUV exposure degrades by formation of carbonyl groups both the PP and the HDPE samples substantially more than the Heat exposure, i.e. the ultraviolet radiation degrades both the PP and the HDPE samples much more than the heat ageing. For long exposure times the Simul exposure with a combination of UV, heat, water spray and freezing according to NT Build 495 [30] falls between the QUV and Heat exposure with respect to degradation strength. Note that the total amount of UV radiation is much larger for the QUV exposure than the Simul exposure, while there is no applied UV radiation during the Heat exposure. Nevertheless, even if it is observed that the UV radiation induces large degradations in both PP and HDPE, it is also observed that heat ageing alone at a constant air temperature of 90 °C (and no UV radiation) causes degradation of PP and HDPE, but as expected at a lower degradation rate.

4.14. Acceleration factor fraction comparisons

For both PP and HDPE the total UV (A + B) exposure after 30 weeks for the QUV ageing is 155 232 Wh/m^2, and 20 790 Wh/m^2 for the Simul ageing, i.e. an UV_{QUV}/UV_{Simul} acceleration factor *fraction* of about 7.47. Assuming an Arrhenius relationship with an assumed activation energy of 70 kJ/mol, a T_{QUV}/T_{Simul} (temperature) acceleration factor *fraction* of about 0.37 is obtained. Hence, a total (simplified) UV and temperature acceleration factor fraction QUV/Simul of 2.8 may be calculated. This total acceleration factor fraction QUV/Simul may be compared with the somewhat lower observed carbonyl formation fractions of approximately 2.6 for PP and 2.2 for HDPE, i.e. 0.275/0.105 and 0.088/0.040 from Fig. 13 for PP and Fig. 14 for HDPE, respectively (at around 1732 or 1734 cm^{-1}). Note that the last measured FTIR spectra for the Heat and Simul exposures show a large increase in the carbonyl absorbance peaks compared to the preceding measurements (e.g. depicted in Figs. 13, 14, 16 and 17). In Fig. 13 induction periods of about 2 weeks for QUV, between 31 and 38 weeks for Heat and between 12 and 30 weeks for Simul are observed for PP. In Fig. 14 induction periods of about 4 weeks for QUV, between 31 and 38 weeks for Heat and between 12 and 30 weeks for Simul are observed for HDPE.

4.15. Some concluding remarks

Thus, with the ATR–FTIR spectroscopical technique, degradation differences in various polymer building materials subjected to different accelerated climate exposures, may be readily investigated. The various accelerated ageing methods and apparatuses have their advantages and disadvantages. For example, the ageing in the QUV apparatus gave a much larger UV exposure than the specific vertical climate simulator (and than the ageing in the heat incubator, naturally). On the other hand, the QUV apparatus did not include freezing/thawing cycles, whereas the specific vertical climate simulator did include freezing/thawing cycles. Horizontal versus vertical sample position may also be important. In some cases it may be beneficial to run ageing experiments in several different apparatuses in order to be able to differentiate the significance of the various ageing exposures.

5. Conclusions

The polymer building materials polypropylene (PP) and high density polyethylene (HDPE) intended for application as water barriers/repellants around building foundation walls have been subjected to various accelerated climate ageing methods which includes exposure to ultraviolet and infrared radiation, heated air, water spray and freezing. Attenuated total reflectance (ATR) Fourier transform infrared (FTIR) radiation spectroscopy has been shown as a powerful and versatile tool in investigating climate ageing processes both qualitatively and quantitatively. The various accelerated ageing apparatuses for degradation of PP and HDPE have been compared, showing some distinct differences. That is, the specific PP samples applied in these experiments were substantially more degraded by formation of carbonyl groups than the specific HDPE samples for all the accelerated climate exposures.

The accelerated ageing methods and apparatuses consisted of a horizontal QUV apparatus including UV and water spray exposure at an elevated temperature, a heat incubator for temperature ageing at an elevated temperature, and finally a vertical climate simulator including UV, IR heat at an elevated temperature, water spray and freezing/thawing exposure. The various accelerated ageing methods and apparatuses have their advantages and disadvantages. For example, the ageing in the QUV apparatus gave a much larger UV exposure than the specific vertical climate simulator. On the other hand, the QUV apparatus did not include freezing/thawing cycles, whereas the specific vertical climate simulator did include many freezing point passes during freezing and thawing. Horizontal versus vertical sample position may also be important. In some cases it may be beneficial to run ageing experiments in several different apparatuses in order to be able to differentiate the significance of the various ageing exposures.

It has been demonstrated that a degradation mechanism of PP and HDPE involves oxidation of the polymer chains by formation of carbonyl groups during accelerated ageing by ultraviolet radiation and exposure to heat.

References

[1] Tylli H, Olkkonen C, Forsskåhl I. A sensitivity analysis of the kinetic mechanism for the photodegradation of a model system of relevance to lignin yellowing. J Photochem Photobio A Chem 1989;49:397–408.

[2] Croll SG, Skaja AD. Quantitative spectroscopy to determine the effects of photodegradation on a model polyester-urethane coating. J Coat Technol 2003;75:85–94.

[3] Gerlock JL, Smith CA, Cooper VA, Dusbiber TG, Weber WH. On the use of Fourier transform infrared spectroscopy and ultraviolet spectroscopy to assess the weathering performance of isolated clearcoats from different chemical families. Polym Degrad Stab 1998;62:225–34.

[4] Rånby B, Rabek JF. Photodegradation photo-oxidation and photostabilization of polymers: principles and applications. John Wiley & Sons; 1975.

[5] Rabek JF. Polymer photodegradation: mechanisms and experimental methods. Chapman & Hall; 1995.

[6] Rabek JF. Photodegradation of polymers: physical characteristics and applications. Springer-Verlag; 1996.

[7] Kumar AP, Depan D, Tomer NS, Singh RP. Nanoscale particles for polymer degradation and stabilization – trends and future perspectives. Prog Polym Sci 2009;34:479–515.

[8] Andrady AL, Hamid HS, Torikai A. Effects of climate change and UV–B on materials. Photochem Photobiol Sci 2003;2:68–72.

[9] Jelle BP, Gustavsen A, Nilsen T-N, Jacobsen T. Solar material protection factor (SMPF) and solar skin protection factor (SSPF) for window panes and other glass structures in buildings. Sol Energy Mater Sol Cells 2007;91:342–54.

[10] Allen NS, Edge M, Ortega A, Sandoval G, Liauw CM, Verran J, et al. Degradation and stabilisation of polumers and coatings: nano versus pigmentary titania particles. Polym Degrad Stab 2004;85:927–46.

[11] Cerruti P, Malinconico M, Rychly J, Matisova-Rychla L, Carfagna C. Effect of natural antioxidants on the stability of polypropylene films. Polym Degrad Stab 2009;94:2095–100.

[12] Commereuc S, Vaillant D, Philippart JL, Lacoste J, Lemaire J, Carlsson DJ. Photo and thermal decomposition of iPP hydroperoxides. Polym Degrad Stab 1997;57:175–82.

[13] Corti A, Muniyasamy S, Vitali M, Imam SH, Chiellini E. Oxidation and biodegradation of polyethylene films containing pro-oxidant additives: synergistic effects of sunlight exposure, thermal aging and fungal biodegradation. Polym Degrad Stab 2010;95:1106–14.

[14] Diepens M, Gijsman P. Photodegradation of bisphenol a polycarbonate with different types of stabilizers. Polym Degrad Stab 2010;95:811–7.

[15] Ding SH, Liu DZ, Duan LL. Accelerated aging and aging mechanism of acrylic sealant. Polym Degrad Stab 2006;91:1010–6.

[16] Forsthuber B, Grüll G. The effects of HALS in the prevention of photodegradation of acrylic clear topcoats and wooden surfaces. Polym Degrad Stab 2010;95:746–55.

[17] Gulmine JV, Akselrud L. FTIR characterization of aged XLPE. Polym Test 2006;25:932–42.

[18] Jelle BP, Nilsen T-N, Hovde PJ, Gustavsen A. Accelerated climate ageing of building materials and application of the attenuated total reflectance (ATR) Fourier transform infrared (FTIR) radiation experimental method. In: Proceedings of the 8th symposium on building physics in the nordic countries, vol. 2, Copenhagen, Denmark, 16–18 June, 2008. Copenhagen: Danish Society of Engineers; 2008. p. 951–8.

[19] Kim M, Pometto III AL, Johnson KE, Fratzke AR. Degradation studies of novel degradable starch-polyethylene plastics containing oxidized polyethylene and prooxidant. J Environ Polym Degrad 1994;2:27–38.

[20] Oliani WL, Parra DF, Otaguro H, Lima LFCP, Lugão AB. Comparative study of polypropylene (HMS–PP) degradation under different conditions. In: Proceedings of the polymer processing society 23rd annual meeting (PPS-23). Salvador, Brazil, May 27–31; 2007.

[21] Pospíšil J, Pilař J, Billingham NC, Marek A, Horák Z, Nešpůrek S. Factors affecting accelerated testing of polymer photostability. Polym Degrad Stab 2006;91:417–22.

[22] Sánchez-Jiménez PE, Pérez-Maqueda LA, Perejón A, Criado JM. A new model for the kinetic analysis of thermal degradation of polymers driven by random scission. Polym Degrad Stab 2010;95:733–9.

[23] Shujun W, Jiugao Y, Jinglin Y. Preparation and characterization of compatible and degradable thermoplastic starch/polyethylene film. J Polym Environ 2006;14:65–70.

[24] Stark NM, Matuana LM. Surface chemistry changes of weathered HDPE/wood–flour composites studied by XPS and FTIR spectroscopy. Poly Degrad Stab 2004;86:1–9.

[25] Szociński M, Darowicki K, Schaefer K. Identification and localization of organic coating degradation onset by impedance imaging. Polym Degrad Stab 2010;95:960–4.

[26] Varghese JK, Na SJ, Park JH, Woo D, Yang I, Lee BY. Thermal and weathering degradation of poly(propylene carbonate). Polym Degrad Stab 2010;95:1039–44.

[27] Wang Z, Wu G, Hu Y, Ding Y, Hu K, Fan W. Thermal degradation of magnesium hydroxide and red phosphorus flame retarded polyethylene composites. Polym Degrad Stab 2002;77:427–34.

[28] Woo L, Ling MTK, Eu B, Sandford C. Application and limitations on thermal and spectroscopic methods for shelf-life prediction. J Therm Anal Calorim 2006;83:131–3.

[29] Woo L, Ling MTK, Eu B, Sandford C. Application and limitations on thermal and spectroscopic methods for shelf-life prediction. Thermochim Acta 2006;442:61–3.

[30] Nordtest Method NT Build 495. Building materials and components in the vertical position: exposure to accelerated climatic strains; 2000.